Materials Letters 79 (2012) 256–258

Contents lists available at SciVerse ScienceDirect

Materials Letters

journal homepage: www.elsevier.com/locate/matlet

Magnetic enhancement of thermal conductivity in copper–carbon nanotube composites produced by electroless plating, freeze drying, and spark plasma sintering

Evan Khaleghi [a,*], Milton Torikachvili [b], Marc A. Meyers [c], Eugene A. Olevsky [a]

[a] Department of Mechanical Engineering, San Diego State University, 5500 Campanile Drive, San Diego, CA 92182-1323, United States
[b] Department of Physics, San Diego State University, 5500 Campanile Drive, San Diego, CA 92182-1233, United States
[c] Mechanical and Aerospace Engineering Department, University of California, San Diego, 9500 Gilman Dr., CA 92037-1441, United States

ARTICLE INFO

Article history:
Received 6 August 2011
Accepted 31 March 2012
Available online 9 April 2012

Keywords:
Magnetic
Carbon nanotube
Spark plasma sintering
Thermal conductivity
Copper
Composites

ABSTRACT

A carbon nanotube and copper composite was synthesized using electroless plating and freeze-drying for green processing, and spark plasma sintering for densification. A magnetic field of 1 T was applied during the freeze-drying process to align the carbon nanotubes along the main axis. Results show that the magnetization process enhanced the alignment and thermal conductivity properties of the final Cu–CNT product (up to 386% in one example), but the properties were lowered overall due to interfacial bonding and particle mixing difficulties, with the results being 5–15% of the thermal conductivity of pure copper.

1. Introduction

Carbon nanotubes (CNTs) have enormous potential in a wide-range of applications due to their high mechanical strength, and unique physical properties [1–4]. There have been many attempts to fabricate composites with CNTs, with metals, ceramics, and polymers as the matrix materials [5–8]. Copper–CNT composites are promising materials for thermal management, due to the potential for high thermal and electrical conductivity [9–12]. The thermal conductivity of an individual multi-walled carbon nanotube is calculated to be greater than 3000 W/m K, while the textbook value for thermal conductivity of pure copper is 400 W/m K [13]. It is desirable to develop a new kind of composite, with the enhanced properties of the carbon nanotube improving the performance of the copper matrix material. This material would have advantages in future thermal management technologies due to its high thermal conductivity, and thermal expansion properties within the range compatible with various electronic circuitry components.

Copper and CNTs are highly insoluble, with CNTs being hardly wet by Cu phase during liquid phase sintering above the melting point of the Cu phase. This is due to the high surface tension of liquid copper, and the smooth, uniform surface of CNTs. It has been shown that CNTs coated with copper by electroless plating could decrease the interface energy between the matrix and the CNTs, increasing the bonding strength, and improving the properties of the whole material. Wang et al. [14] and Shi et al. [15] successfully used electroless plating to coat CNTs and create composites with copper. Others [16–18] used various other techniques to create the composites, but were not as successful as electroless plating.

In this paper, an investigation into the creation of high performance Cu–CNT composites is described. The composites are fabricated using electroless plating of copper onto the CNTs, using uniaxial freeze-drying as the main dispersion mechanism, and using magnetic alignment [19–21] of the CNTs to further enhance final properties. This is the first application of uniaxial freezing to this material system, and the primary purpose of using this process is twofold — to use the uniaxial ice crystal growth to encourage alignment of the carbon nanotubes in the axial direction, and also to help disperse the carbon nanotubes in the copper matrix. The Cu–CNT green bodies produced based on this approach have been consolidated by spark-plasma sintering — a powder consolidation technique with the potential of preserving the material structure properties created during the green processing stage.

2. Materials and methods

Multi-walled carbon nanotubes (Cheap Tubes, Inc., USA) were electroless plated with copper. First, the surface of the carbon nanotubes was functionalized by soaking them in 10% nitric acid for 8 h at room temperature, followed by rinsing thoroughly with DI water, and then drying in a furnace at 60 °C. Following the work of Shi et al. [15], we then used $CuSO_4$ at a concentration of 12–15 g/L, $EDTANa_2$

* Corresponding author.
E-mail address: ekomega@yahoo.com (E. Khaleghi).

0167-577X/$ – see front matter © 2012 Elsevier B.V. All rights reserved.
doi:10.1016/j.matlet.2012.03.117

at a concentration of 25–30 g/L, NaOH at a concentration of 16 g/L with additional amounts used to maintain pH, HCHO at a concentration of 30 g/L, and Na_2SO_4 at a concentration of 40 g/L chemicals in a 50 mL bath (all chemicals from Fisher Scientific, USA), to precipitate copper onto the surface of the MWCNTs. A pH of 12 was maintained throughout the process through careful addition of NaOH and monitoring with a pH meter, as other research [15] has shown that this is optimal for deposition. A one-step method was utilized, along the lines of Ang et al. [22] as this showed superior results and faster production times compared to a traditional two-step method.

4.5 and 4.25 g of 99.9% pure copper powder (particle size −325 mesh) (Alfa Aesar, USA) were mixed with .5 and .75 g of copper coated multi-walled carbon nanotubes, to produce specimens with 10 and 15 wt.% CNTs, respectively. We chose these weight fractions for the CNTs due to preliminary research which showed that these concentrations would be suitable for increasing the thermal conductivity while also being easily dispersed throughout the copper matrix. The powders were mixed ultrasonically in ethanol (Fisher Scientific, USA) for 20 min, and .05 g of sodium dodecyl sulfate dispersant (Fisher Scientific, USA) was added to discourage agglomeration.

The resultant solution was poured into a graphite SPS die (Electrodes, Inc., USA) for the uniaxial freezing process, as per previous research [23,24]. The graphite die was located in an aluminum holder, surrounded by liquid nitrogen, and the powder slurry was poured directly into the die. For the magnetic specimens, magnets were placed on the top and bottom surfaces of the die, with their fields aligned, as shown in Fig. 1. The field strength of each magnet was approximately 0.5 T, for a combined total of 1 T applied to the specimen.

After uniaxial freezing was completed, the powder/die combination was freeze-dried to remove water before sintering. Spark Plasma Sintering was then conducted in a Dr. Sinter Lab 515s (SPS Syntex, Co., Japan) to densify the specimens, using the same die as for all previous processing.

The spark plasma sintering profile used for all specimens was 7 min to 700 °C (100 °C/min), hold for 8 min, with 50 MPa applied pressure, as we found this produced 100% fully dense specimens of pure copper.

Specimens were sectioned into 1.5 mm by 1.5 mm by 8 mm slices for use with the Thermal Transport Option of Quantum Design's Physical Property Measurement System PPMS-9 to measure thermal conductivity. Thermal conductivity is measured in this device by monitoring the temperature drop across the sample as a known amount of heat travels from the hot to the cold section.

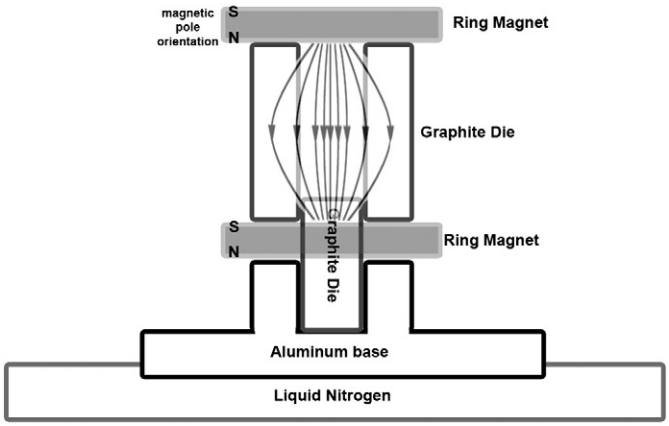

Fig. 1. A diagram of the die setup and magnetic field flow during uniaxial freeze-drying of the Cu–CNT powder.

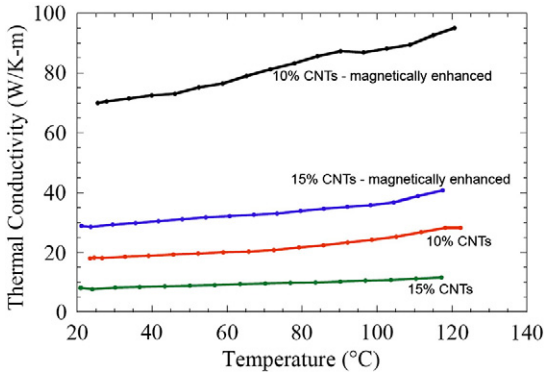

Fig. 2. The thermal conductivity of copper–CNT composite specimens is plotted vs. temperature.

3. Results

Fig. 2 shows the thermal conductivity of the four composite specimens in a range of temperatures of interest to the semiconductor industry (20–120 °C). Table 1 shows the comparison of the room temperature (20 °C) thermal conductivity of the four composite specimens compared to pure copper. One can see that the composite specimens show severely decreased thermal conductivity compared to the pure material, similar to the results obtained by Edtmaier et al. [16]. Fig. 2 also shows a decrease in thermal conductivity with increasing CNT concentration (10 to 15 wt.%), with a 41 W/m K difference for the magnetically-processed specimens, and a 10 W/m K difference for the non-magnetically processed specimens.

The most important aspect is the increase in thermal conductivity for specimens where the magnetic field was applied. Both the freeze-drying and magnetic field were used in an attempt to align the CNTs along the axial direction, so that their superior anisotropic thermal conductivity would provide a benefit to the copper matrix. The application of the magnetic field clearly enhanced the thermal conductivity of the produced specimens, with an increase of approximately 52 W/m K (386%) for the 10% specimens, and an increase of approximately 21 W/m K (361%) for the 15% specimens.

Optical microscopy images (Fig. 3) show some orientation and directionality of the CNT agglomerates in the 15% magnetically-processed specimen, as opposed to the similar composition specimen created without magnets.

This orientation enhancement from the magnetic field is the likely cause of the thermal conductivity enhancement compared to the non-magnetically enhanced specimens, although due to the agglomeration of the CNTs and interfacial energy issues, the measured values are lower than pure copper.

Electron microscopy images also show the boundaries between the CNT agglomerates and the bulk copper matrix. One can see from Fig. 4 that there is a clear boundary between CNTs and copper, the presence of which is known to significantly reduce the thermal conductivity of these types of composites. An ideal composite would

Table 1
The thermal conductivity of Cu–CNT composites compared to pure copper, at room temperature.

Material	Cu + 10% CNTs	Cu + 10% CNTs-magnetically enhanced	Cu + 15% CNTs	Cu + 15% CNTs-magnetically enhanced	Pure copper
Thermal conductivity (W/m K)	18.12	70.01	8.03	28.96	400.0

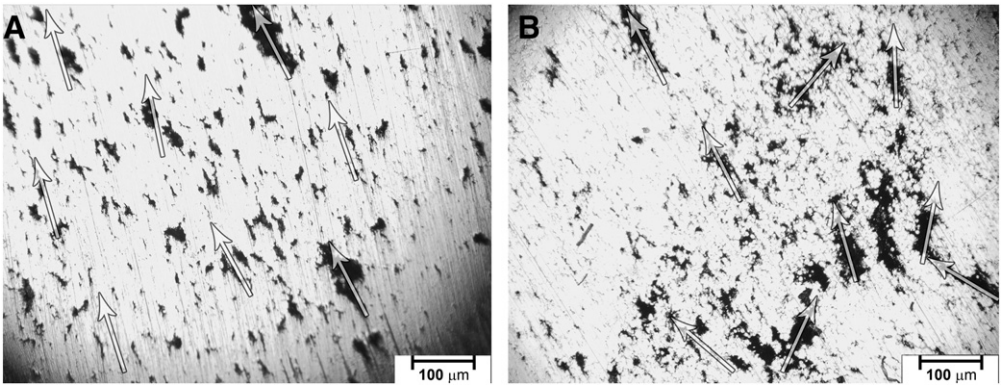

Fig. 3. (A) The 15% CNT–Cu magnetically enhanced specimen shows some preferred orientation toward the upper left corner of the image. (B) The 15% CNT–Cu specimen does not show the same orientation bias. Both images are taken at 100× magnification.

have individual carbon nanotubes dispersed uniformly throughout the metal matrix, unlike in the figure.

We can predict the thermal conductivity of the matrix with high interfacial resistance by comparing the system to a porous copper specimen, where the "pores" would be the clusters of CNTs. Ondracek and Schulz created an equation for calculating this thermal conductivity [25]:

$$\lambda/\lambda_0 = (\lambda - P)/(1 - \beta P)$$

where λ is the thermal conductivity of the porous specimen, λ_0 is the porosity of the pure specimen, P is the porosity, and β is a factor related to the shape of the pores. β is 0.5 for spherical pores that are non-conductive. Using the conductivity of copper, 0.5 as an extreme estimate for β, and the calculated porosity for our two specimens (based on volume fraction), we expect the thermal conductivity of the 10% specimen to be 230 W/m K, and the 15% specimen to be 183 W/m K. These values are significantly higher than the experimental values, and we would have to increase the approximation β to 8.5 to approach the experimental values. This would correspond to pores which are extremely long and thin, which are not present in the SEM images.

4. Conclusions

Magnetic enhancement of the processing of the copper–carbon nanotube composites helps to align the carbon nanotubes and improve thermal conductivity by as much as 386% (18.12 to 70.01 W/m K) compared to similar specimens processed without magnetic fields. However, significant reduction in thermal conductivity, relative to pure copper, is noted due to agglomeration of coated CNTs in the metal matrix. Uniaxial freeze-drying showed no ability to improve thermal conductivity, either through nanotube alignment, or otherwise, and may decrease it (although the mechanism is still not clear).

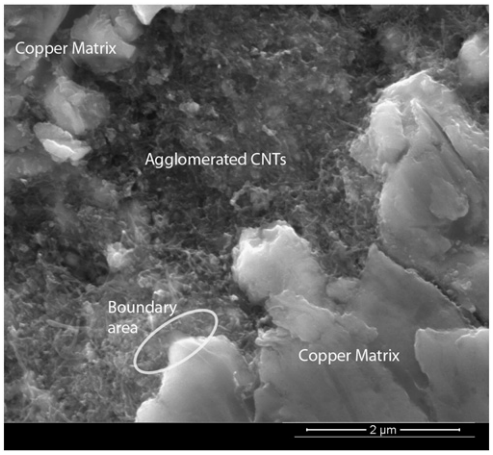

Fig. 4. A clear boundary can be seen between the CNTs and the copper in this 15%-CNT–Cu specimen, indicating interfacial boundary problems.

Acknowledgments

The support of the National Science Foundation (NSF Grant No. DMR-0805335) and the NSF Division of Civil, Mechanical, and Manufacturing Innovations (Grant CMMI-0758232) is gratefully acknowledged. The authors acknowledge the assistance of Dr. Steve Barlow, and use of equipment at the San Diego State University Electron Microscopy Facility acquired by NSF instrumentation grant DBI-0959908.

References

[1] Baughman RH, Zakhidov AA, de Heer WA. Science 2002;297:787–92.
[2] Avouris P. Chem Phys 2002;281:429–45.
[3] Graham AP, Duesberg GS, Seidel R, Liebau M, Unger E, Kreupl F, et al. Diamond Relat Mater 2004;1:1296–300.
[4] Hu CG, Wang WL, Wang SX, Zhu W, Li Y. Diamond Relat Mater 2003;12:295–1299.
[5] Deng CF, Wang DZ, Zhang XX, Lia B. Mater Sci Eng A 2007;444:138–45.
[6] Gao L, Jiang L, Sun J. J Electroceram 2000;17:51–5.
[7] Bian Z, Zhang T, Inoue A. Mater Trans 2004;45:284–7.
[8] Miyagawa H, Misra M, Mohanty AK. J Nanosci Nanotechnol 2005;5:1593–615.
[9] Yoon ES, Lee JS, Oh ST, Kim BK. Int J Refract Met Hard Mater 2002;20:201–6.
[10] Hong SH, Kim BK. Mater Lett 2003;57:2761–7.
[11] Ryu SS, Kim YD, Moon IH. J Alloys Compd 2002;335:233–40.
[12] Doré F, Lay S, Eustathopoulos N, Allibert CH. Scr Mater 2003;49:237–42.
[13] Parker WJ, Jenkins RJ, Butler CP, Abbott GL. J Appl Phys 1961;32:1679–84.
[14] Wang F, Arai S, Endo M. Electrochem Commun 2004;6:1042–4.
[15] Shi XL, Yang H, Shao GQ, Duan XL, Yan L, Xiong Z, et al. Mater Sci Eng A 2007;457:18–23.
[16] Edtmaier C, Janhsen T, Hula RC, Pambaguian L, Wulz HG, Forero S, et al. Adv Mater Res 2009;59:131–7.
[17] Xu L, Chen X, Pan W, Li W, Yang Z, Pu Y. Nanotechnology 2007;18:435607.
[18] Wu HX, Cao WM, Li Y, Liu G, Wen Y, Yang HF, et al. Electrochim Acta 2010;55:3734–40.
[19] Islam MF, Milkie DE, Torrens ON, Yodh AG, Kikkawa JM. Phys Rev B 2005;71:201401(R).
[20] Chen RB, Chang CP, Hwang JS, Chuu DS, Lin MF. J Phys Soc Jpn 2005;74:1404–7.
[21] Okada S, Oshiyama A. J Phys Soc Jpn 2003;72:1510–5.
[22] Ang LM, Hor TSA, Xu GQ, Tung CH, Zhao SP, Wang JLS. Carbon 2000;38:363–72.
[23] Song KH, Liu HK, Dou SX, Sorrell CC. J Am Ceram Soc 1990;71:1771–3.
[24] Fukusawa ZY, Deng M, Ando T, Ohji S, Kanzaki T. J Am Ceram Soc 2002;85:2151–5.
[25] Ondracek G, Schulz B. J Nucl Mater 1973;46:253–8.